Eur. Phys. J. E (2015) **38**: 132
DOI 10.1140/epje/i2015-15132-2

THE EUROPEAN PHYSICAL JOURNAL E

Regular Article

Study of critical dynamics in fluids via molecular dynamics in canonical ensemble

Sutapa Roy and Subir K. Das[a]

Theoretical Sciences Unit, Jawaharlal Nehru Centre for Advanced Scientific Research, Jakkur P.O, Bangalore 560064, India

Received 21 August 2015 and Received in final form 11 November 2015
Published online: 23 December 2015 –

Abstract. With the objective of understanding the usefulness of thermostats in the study of dynamic critical phenomena in fluids, we present results for transport properties in a binary Lennard-Jones fluid that exhibits liquid-liquid phase transition. Various collective transport properties, calculated from the molecular dynamics (MD) simulations in canonical ensemble, with different thermostats, are compared with those obtained from MD simulations in microcanonical ensemble. It is observed that the Nosé-Hoover and dissipative particle dynamics thermostats are useful for the calculations of mutual diffusivity and shear viscosity. The Nosé-Hoover thermostat, however, as opposed to the latter, appears inadequate for the study of bulk viscosity.

1 Introduction

In the vicinity of a critical point [1], various static [1–3] and dynamic [3–11] quantities exhibit power-law singularities. Computer simulations played a crucial role in the understanding of static critical phenomena [12]. In dynamics, on the other hand, simulations are recent, particularly for fluid criticality. In this case, in addition to the finite-size effects, critical slowing down poses enormous difficulty. Note that the slowest relaxation time, $\tau_{\rm max}$, diverges at the criticality as [3, 12]

$$\tau_{\rm max} \sim L^z, \tag{1}$$

where L is the linear dimension of the system and z is a dynamic critical exponent. While in the static critical phenomena, the problem of critical slowing down can be significantly reduced via a smart choice of ensemble (with smaller value of z), in dynamics this is not possible. The liberty in statics stems from the robust universality of static critical phenomena.

For the computational study of critical dynamics in fluids, using microscopic models, one typically carries out molecular dynamics (MD) [13–15] simulations. Usually one considers the microcanonical ensemble (constant N, V, E, which are, respectively, the total number of particles, confining volume and energy) where requirements of hydrodynamics are satisfied. However, as seen in eq. (1), close to the critical point, overwhelmingly long simulation runs are required to avoid finite-size effects even at a moderate level. In such a situation, control of temperature (T) in the NVE ensemble becomes problematic. A representative case for temperature drift in microcanonical runs has been shown in fig. 1. Drift of such magnitude is acceptable in the normal region of the parameter space, *i.e.*, far away from any phase transition. However, close to the critical point, where one focuses on quantifying singular behavior, this becomes problematic. This calls for the study of fluid critical dynamics in canonical (NVT) ensemble where, instead of E, T is kept constant.

Various thermostats [13,14] are used to maintain temperature in MD simulations in NVT ensemble, *e.g.* Andersen thermostat (AT), Langevin thermostat (LT), Nosé-Hoover thermostat (NHT), dissipative particle dynamics thermostat (DPDT), etc. Even though most of the thermostats are useful in controlling the temperature of the system, only a few are appropriate for the calculation of transport properties in fluids. Crucial tests of a thermostat, in terms of providing the correct value of a transport quantity as well as in keeping the temperature constant, lie in nontrivial phenomena like phase transition dynamics. In a recent work [16], we have demonstrated the usefulness of the NHT for the calculation of shear viscosity. In this paper we address this issue in a more general context.

In AT [13], the temperature is controlled via the random assignments of velocities to a fraction of particles according to the Maxwell distribution, mimicking collisions of the particles with a heat bath. Due to this Monte Carlo-like stochastic nature, AT is not useful for the calculation of transport properties in fluids. With increasing collision frequency, the transport coefficients deviate further and further from the desired value. This stochastic character is also true for LT.

[a] e-mail: das@jncasr.ac.in

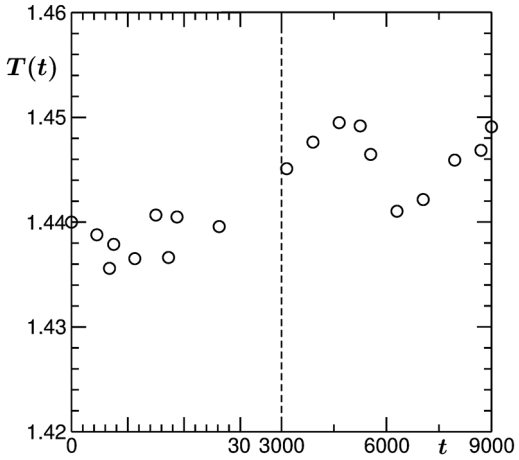

Fig. 1. Drift of temperature is demonstrated for a typical molecular dynamics run in microcanonical ensemble. The cubic simulation box has a linear dimension $L = 14$ and number of particles 2744. The initial temperature is set to 1.44, very close to the critical value.

For MD in NVE ensemble, one solves Newton's equations of motion involving the inter-particle force. Like AT, in the NVT ensemble, depending upon the thermostat, additional rules are imposed. In the case of LT, an additional drag force proportional to the velocity is introduced, in addition to a random force, both coming from the background solvent particles. There, for the i-th particle, one solves the equation [17]

$$\frac{\mathrm{d}^2\vec{r}_i}{\mathrm{d}t^2} = -\vec{\nabla}U_i - \gamma\frac{\mathrm{d}\vec{r}_i}{\mathrm{d}t} + \vec{W}_i, \tag{2}$$

where $\vec{r}_i$ is the position of the particle, U_i is the inter-particle potential, t is the time, γ the drag coefficient and $\vec{W}_i$ is a temperature-dependent Gaussian noise with mean zero. The noise correlation between two times t and t' follows the fluctuation-dissipation relation

$$\langle W_{i\mu}W_{j\nu}\rangle = 2k_BT\gamma\delta_{ij}\delta(t-t')\delta_{\mu\nu}. \tag{3}$$

In eq. (3), μ and ν correspond to the Cartesian axes of space coordinates and k_B is the Boltzmann constant. In case of non-Gaussian noise, one needs to appropriately adjust the numerical factor in eq. (3). In this work we have used uniform random numbers between -1 and 1, thus the prefactor 2 is replaced by 6.

Due to their inability to conserve the local momentum, AT and LT are used only for the equilibration purpose. Nevertheless, for the sake of completeness, we will present some results using these thermostats as well. There exist a number of thermostats, *e.g.* NHT, DPDT, etc., that are believed to be good for the calculation of transport properties in fluids. The understanding of the usefulness of these thermostats, however, to the best of our knowledge, is essentially restricted to the single-particle dynamics.

In DPDT [18–20], the dissipative force in eq. (2) is given by $\gamma\omega^D(r_{ij})(\vec{v}_{ij}\cdot\vec{e}_{ij})\vec{e}_{ij}$ where $\vec{r}_{ij}$ and $\vec{v}_{ij}$ are, respectively, the relative position and velocity between i and j particles with $\vec{e}_{ij} = \vec{r}_{ij}/r_{ij}$; $r_{ij} = |\vec{r}_{ij}| = r$. Here, ω^D is a weight function connected to the random force as $\sqrt{2\gamma k_BT\omega^D}\omega_{ij}\vec{e}_{ij}$, where ω_{ij} are random numbers with $\omega_{ij} = \omega_{ji}$. For the choice of ω^D, there is no fixed prescribed rule. In this work we use [21] $\omega^D = (1-r)^2$ for $r \leq 1$ and 0 otherwise. From the property of the random force and the expression of the dissipative force, it is understandable that DPDT will preserve local momentum, thus hydrodynamics. However, this thermostat has issues related to keeping the temperature constant. For the choice of the weight function mentioned above and $\gamma = 0.1$, we obtained a reasonable temperature control in this work. Note that for LT we used $\gamma = 1$.

In NHT, an additional degree of freedom Ξ is introduced and one solves the equations [13]

$$\dot{m_i\vec{r}_i} = \vec{p}_i, \tag{4}$$

$$\dot{\vec{p}}_i = -\frac{\delta U_i}{\delta\vec{r}_i} - \Xi\vec{p}_i, \tag{5}$$

$$\dot{\Xi} = \left(\sum_{i=1}^{N} p_i^2/m_i - 3N/\beta\right)\Big/Q, \tag{6}$$

where $\beta = 1/k_BT$, Ξ is a time-dependent drag, $\vec{p}_i$ is the momentum and Q is the coupling strength between the system and the thermostat. Essentially, in this case, the simulation is done in microcanonical ensemble [13,18] with a modified Hamiltonian that provides averages equivalent to those of a canonical ensemble with the original Hamiltonian. The original energy function, that is constant in microcanonical ensemble, fluctuates in this method, as in the canonical ensemble. The constant of motion here is related to the Helmholtz free energy. Unless otherwise mentioned, for all our presented results the value of Q was set to unity.

As is clear by now, in this paper we provide results for the utility of NHT and DPDT with respect to the study of dynamic critical phenomena. Despite its problems related to local momentum conservation, NHT still remained popular for the study of transport using NVT ensemble. Of course, every hydrodynamic-preserving thermostat has some disadvantages, *e.g.*, DPDT suffers from the temperature control problem.

The rest of the paper is organized as follows. In sect. 2, we introduce the model. The results are presented in sect. 3. Finally, the paper is concluded in sect. 4 with a summary and discussion.

2 Model and phase behavior

In our binary $(A + B)$ mixture model [22–24], particles interact via the Lennard-Jones (LJ) pair potential

$$u(r) = 4\varepsilon_{_{\alpha\beta}}\left[\left(\frac{\sigma}{r}\right)^{12} - \left(\frac{\sigma}{r}\right)^{6}\right], \tag{7}$$

where σ is the particle diameter and $\varepsilon_{\alpha\beta}\,[\alpha,\beta = A,B]$ is the interaction strength. For the sake of computational convenience, we have introduced a cut-off and shifting of

Table 1. Values of critical temperatures for different system sizes.

L	8	10	12	14	16	∞
T_c^L	1.461	1.447	1.440	1.436	1.433	$T_c \simeq 1.421$

the potential to zero at $r_c = 2.5\sigma$. This, however, introduces a discontinuity in the force at r_c, which was removed by adding a term [14] $(r - r_{_c})(\mathrm{d}u/\mathrm{d}r)_{r=r_{_c}}$. We work with a symmetric model by setting $\varepsilon_{_{AA}} = \varepsilon_{_{BB}} = 2\varepsilon_{_{AB}} = \varepsilon$ which produces liquid-liquid phase separation. The overall density of particles was set to unity. This avoids overlap between liquid-liquid and vapor-liquid phase separations.

The phase diagram for this model was studied [22–24] via a semi grandcanonical Monte Carlo (MC) [12, 13] method. In this scheme, in addition to the standard particle displacement moves, one tries identity switches $A \to B \to A$ which are accepted or rejected according to the standard Metropolis criterion. For the identity moves it is necessary to include in the Boltzmann factor [13] the chemical potential difference between the two species. This difference, however, is zero along coexistence and for $50 : 50$ composition above the critical temperature T_c, due to the symmetry of the model. In this ensemble, from the fluctuation of concentration x_α $(= N_\alpha/N$, N_α being the number of particles of species $\alpha)$, one obtains a probability distribution $P(x_\alpha)$. Below the critical temperature, $P(x_\alpha)$ should have a two-peak structure, the locations of the peaks providing the points along the coexistence. At the critical temperature, the form of the distribution crosses over from the double peak to a single peak one. But, this critical temperature is system-size-dependent that we will denote as T_c^L, which, in the limit $L \to \infty$, will converge to the thermodynamic critical temperature, T_c. In table 1 we list the values of T_c^L for a few system sizes [24, 25].

As already mentioned, transport properties are studied via MD simulations in NVE as well as NVT ensembles, for the latter various temperature controlling methods, discussed in the previous section, were used. Details on the calculation of transport properties will be provided in the next section.

All our simulations were performed in three space dimensions with cubic boxes of linear size L (in units of σ) and periodic boundary conditions in all directions. The equations of motion in MD were solved by applying Verlet velocity algorithm with integration time step $\Delta t = 0.005 t_0$, the LJ time unit t_0 to be defined soon. Before starting the production runs, the configurations were equilibrated via MC simulations and, in the case of MD in NVE ensemble, further thermalization runs were performed via MD with AT. Except for self-diffusivity, results are presented after averaging over a very large number of independent initial configurations, ranging between 80 and 640. In case of self-diffusivity, this number is 5. For collective properties, as the terminology suggests, such high numbers become necessary due to lack of averaging involving the individual particles.

3 Results

Using MD, at various temperatures (fixing the composition to the critical value) we present results for the self-diffusivity (D), Onsager coefficient ($\mathscr{L}$), shear viscosity (η) and bulk viscosity (ζ). These quantities were calculated (in dimensionless units) from the Green-Kubo (GK) relations [26] as (note that, because of the symmetry of the model $D = D_A = D_B$, D_α being the self-diffusivity of species α)

$$D(t) = \left(\frac{t_0}{3\sigma^2}\right) \int_0^t \mathrm{d}t' \big\langle \vec{v}_{i,\alpha}(t') \vec{v}_{i,\alpha}(0) \big\rangle, \tag{8}$$

$$\mathscr{L}(t) = \left(\frac{t_0 \varepsilon}{3 k_{_B} N T \sigma^2}\right) \int_0^t \mathrm{d}t' \big\langle \vec{J}_{_{AB}}(t') \vec{J}_{_{AB}}(0) \big\rangle, \tag{9}$$

$$\eta(t) = \left(\frac{t_0^3 \varepsilon}{\sigma V T m^2}\right) \int_0^t \mathrm{d}t' \big\langle P_{\mu\nu}(t') P_{\mu\nu}(0) \big\rangle, \tag{10}$$

and

$$Y(t) = \left(\frac{t_0^3 \varepsilon}{\sigma V T m^2}\right) \int_0^t \mathrm{d}t' \big\langle P'_{\mu\mu}(t') P'_{\mu\mu}(0) \big\rangle, \tag{11}$$

where t_0 is the LJ time unit $(= \sqrt{m\sigma^2/\varepsilon}\,)$ and m is the particle mass (same for all particles in our model). In eq. (9), $\vec{J}_{AB}$ is a concentration current defined as

$$\vec{J}_{_{AB}}(t) = x_{_B} \sum_{i=1}^{N_A} \vec{v}_{_{i,A}}(t) - x_{_A} \sum_{i=1}^{N_B} \vec{v}_{_{i,B}}(t), \tag{12}$$

$\vec{v}_{_{i,\alpha}}$ being the velocity of the i-th particle of species α. In eq. (10), $P_{\mu\nu}$ are the off-diagonal elements of the pressure tensor given as [26]

$$P_{\mu\nu}(t) = \sum_{i=1}^{N} \left[m v_{i\mu} v_{i\nu} + \frac{1}{2} \sum_{j(\neq i)} (\mu_i - \mu_j) F_\nu(|\vec{r}_i - \vec{r}_j|) \right], \tag{13}$$

$\vec{F}$ being the force between particles i and j; μ_i is a Cartesian coordinate for the position of particle i. In eq. (11), $Y = \zeta + \frac{4}{3}\eta$ and $P'_{\mu\mu} = P_{\mu\mu} - P$, P being the pressure.

These quantities can also be calculated from the corresponding mean squared displacements (MSD) following the Einstein relations, *e.g.* the self-diffusivity D, the Onsager coefficient $\mathscr{L}$ and the shear viscosity η are calculated as [26]

$$D(t) = \left(\frac{t_0}{6t\sigma^2}\right) \big\langle \big|\vec{r}_{i,\alpha}(t) - \vec{r}_{i,\alpha}(0)\big|^2 \big\rangle, \tag{14}$$

$$\mathscr{L}(t) = \left(\frac{t_0 N_A^2 \varepsilon}{6 k_{_B} t N T \sigma^2}\right) \big\langle \big|\vec{R}_{_A}(t) - \vec{R}_{_A}(0)\big|^2 \big\rangle, \tag{15}$$

and

$$\eta(t) = \left(\frac{t_0^3 \varepsilon}{2 k_{_B} t V \sigma T m^2}\right) \big\langle \big|Q_{_{xy}}(t) - Q_{_{xy}}(0)\big|^2 \big\rangle. \tag{16}$$

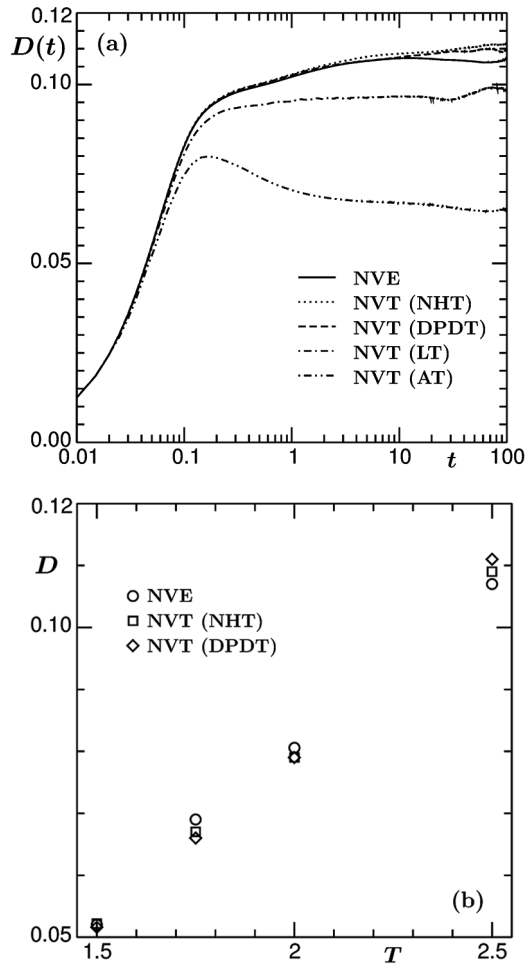

Fig. 2. (a) Plot of time-dependent self-diffusivity obtained using various ensembles. (b) Plot of $D\,[D(\infty)]$ *vs.* T, for NVE, NHT and DPDT. All results are obtained after averaging over 5 independent initial configurations.

In eq. (15), $\vec{R}_\alpha$ is the centre of mass (CM) coordinate of species α and in eq. (16), the generalized displacement Q_{xy} has the expression

$$Q_{xy}(t) = \sum_{i=1}^{N} x_i(t) v_{iy}(t). \tag{17}$$

In the rest of the paper, we set m, ε, σ, t_0 and k_B to unity. For self-diffusivity, Onsager coefficient and shear viscosity, we present results from the MSD relations whereas the results for bulk viscosity were obtained using the GK relation.

We start by showing a comparison of the time-dependent self-diffusivity, calculated from the Einstein relation, in fig. 2(a), obtained from NVE and NVT ensembles, at $T = 2.5$. For NVT ensemble we have included results from AT, LT, NHT and DPDT as temperature controller. As expected, AT and LT do not provide results consistent with the NVE one. However, the results from NHT and DPDT are very much in agreement with the latter. The final values of the transport quantities, here and in other

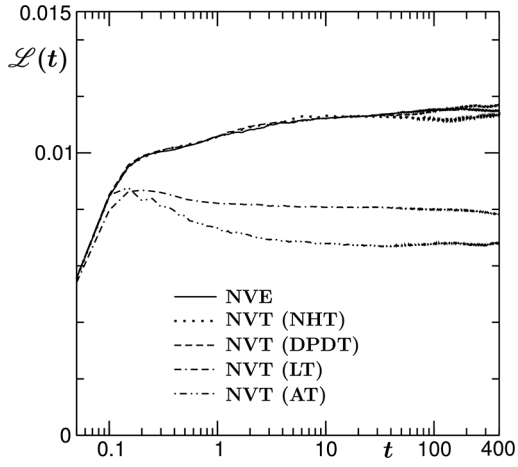

Fig. 3. Plot of Onsager coefficient as a function of time, from MD calculations in NVE and NVT ensembles. For NVT ensemble, as indicated, four different thermostats were used. In all the cases, values of T and L were set to 2.5 and 10, respectively.

places, are obtained from the flat portions of these time-dependent plots. In fig. 2(b) we show a comparison of D calculated from NVE, NHT and DPDT, as a function of temperature, along the critical (50 : 50) composition line. All are in good agreement (the observed differences are not systematic). This is expected and demonstrated earlier [13]. However, the cases of collective properties (except for shear viscosity, via NHT, in a recent work [16]) are missing in the literature which we address below.

In fig. 3 we show a comparison similar to fig. 2(a) but for the time-dependent Onsager coefficient. For NHT, even though we have presented the result using only $Q = 1$, we have performed the calculations with values of Q up to 100 and observed that the results are not very sensitive to the choice of this parameter. This fact will be demonstrated later, for all the transport quantities, by presenting representative results using the optimum value [27] of Q ($\approx 6Nk_BT/\omega_0^2$, ω_0 being a characteristic vibrational frequency whose value is approximately 10 for typical LJ fluid). Again, very good agreement is observed for results from NVE, NHT and DPDT. In the following we focus on the critical behavior of this quantity.

Note that $\mathscr{L}$ is expected to diverge at criticality with the correlation length ξ as [3]

$$\frac{\mathscr{L}}{T} \sim \xi^{x_\lambda}, \tag{18}$$

with $x_\lambda \simeq 0.9$. To verify the consistency of our simulation results with this number for the critical exponent, we take the route of finite-size scaling analysis [28]. Noting that at criticality ξ scales with L, for results obtained at T_c^L,

$$\frac{\mathscr{L}}{T} \sim L^{x_\lambda}. \tag{19}$$

It was observed in previous NVE MD simulations of this model [22,23] that $\mathscr{L}$ has a strong background contribution $\mathscr{L}_b$. The value of $\mathscr{L}_b$ was estimated to be $\simeq 0.0033$,

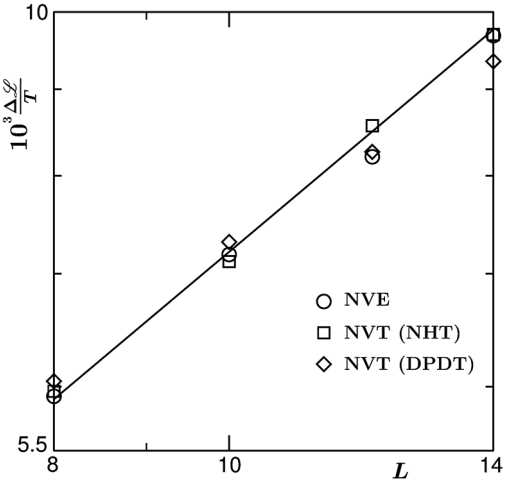

Fig. 4. A finite-size scaling plot of Onsager coefficient [$\mathscr{L} = \mathscr{L}(\infty)$], after subtracting the background contribution, using data at T_c^L. Results from both NVE and NVT ensembles are shown. For NVT ensemble, we have included data from NHT and DPDT. The continuous line corresponds to the theoretical prediction for critical divergence.

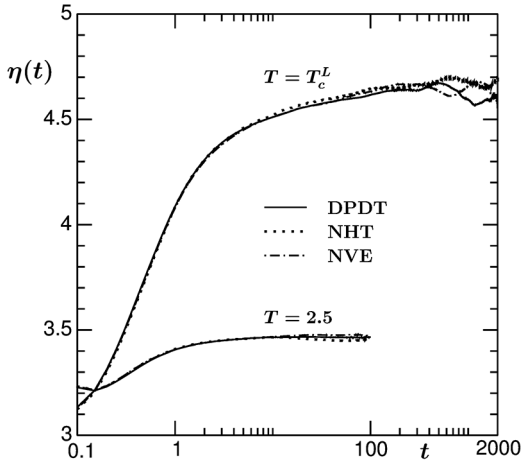

Fig. 5. Plot of shear viscosity as a function of time for two different temperatures, viz., $T = 2.5$ and $T = 1.447$, the latter being the value of T_c^L for $L = 10$, the system size for which the results are presented. We have shown results from NVE, NHT and DPDT calculations.

a reasonably large number, given that for small system sizes this number can be comparable to the total value. We will thus deal with the critical part $\Delta\mathscr{L}(= \mathscr{L} - \mathscr{L}_b)$ only. So, when calculated at T_c^L, a plot of $\Delta\mathscr{L}/T$ *vs.* L will be consistent with a power-law with exponent 0.9. This is demonstrated in fig. 4. Note that we have shown results from NHT, DPDT, as well as from NVE ensemble. All of them are in good agreement. This essentially demonstrates that NHT and DPDT are good devices for the calculation of mutual diffusivity (D_{AB}) even for quantitative understanding of critical dynamics. Here note that $D_{AB} = \mathscr{L}/\chi$, where χ is the concentration susceptibility that can be conveniently calculated from concentration fluctuation in MC simulations outlined above. Sightly poorer agreement of the DPDT data with the expected theoretical behavior, compared to NHT ones, is due to the temperature control problem that this method suffers from, in the long run.

Having demonstrated the usefulness of NHT and DPDT in the calculation of the diffusion constants, we turn our attention to viscosities. In fig. 5 we show the time-dependent shear viscosity, using the Einstein relation, for NVE, NHT and DPDT. Two different temperatures are included, viz., $T = 2.5$ and $T = 1.447$. Here we do not show the results obtained using AT and LT which, as we have already understood and as is known, are not appropriate for the study of transport properties in fluids. For both NHT and DPDT, satisfactory agreement is achieved with the NVE calculation. In our recent work [16], agreement between the NHT and NVE was established. There our estimations of the corresponding critical exponent via these two methods agreed nicely with each other. However, in that work, DPDT was not applied. Having demonstrated the expected usefulness of DPDT, for this purpose, we move to the case of bulk viscosity. For bulk viscosity we avoid demonstrating the critical divergence, by keeping the difficulty in estimation of this quantity in mind. One of the primary difficulties lies in the estimation of P that needs to be subtracted from the diagonal elements of the pressure tensor. Even a slight error in this quantity can lead to a misleading number in the final value. This, however, in our calculations was appropriately taken care of. Here note again that, for all the collective transport properties discussed in this work, the critical divergences were estimated from calculations via MD in NVE ensembles and the results are in good agreement with existing theoretical predictions. Due to the above-mentioned difficulty and diverging relaxation time, it becomes inevitable to choose temperatures reasonably far away from the critical value, for the bulk viscosity.

Even though so far it appears that the NHT is a good tool to study dynamic critical phenomena, in fact better than the DPDT, from the temperature control point of view, we have encountered problem in obtaining the correct value of bulk viscosity with this thermostat, at least for this value of the coupling constant. In fig. 6 we show time-dependent bulk viscosity. Good agreement (within 10%) is obtained between NVE and DPDT for two different temperatures. However, note that, possibly due to temperature fluctuation/drift, the agreement between NVE and DPDT is not good if data from later parts of the runs are considered for the calculation. This is despite the fact that for this particular calculation we have used $\gamma = 0.001$. The choice of a smaller value of γ has a connection with adopting smaller integration time steps. From a previous simulation [19], it was reported that temperature destabilizes with the increase of Δt. As already mentioned, unlike other quantities, for ζ, the error in the calculation of P brings additional problem, which enhances further if there is a strong temperature fluctuation or a drift. A further comparison of time-dependent

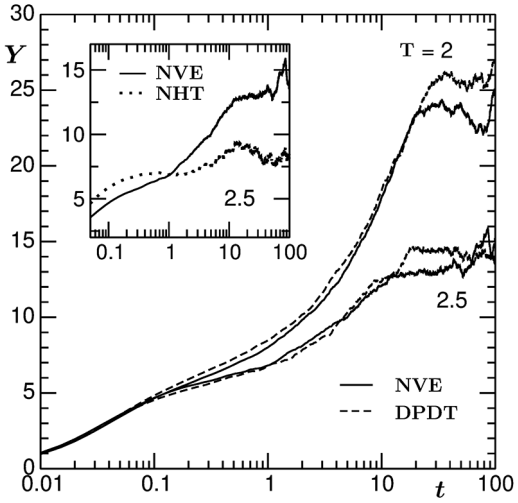

Fig. 6. Comparison of time-dependent bulk viscosity for calculations from NVE and DPDT, at two different temperatures. The inset shows a comparison between NVE and NHT for this quantity, only at $T = 2.5$.

bulk viscosity is shown in the inset of fig. 6, using data from NVE and NHT calculations. Clearly, NHT provides a misleading value. In fact there is disagreement between the two calculations starting from the very early time.

4 Conclusion

In this paper we presented comparative results for transport properties in a binary fluid mixture obtained from molecular dynamics [13] calculations in microcanonical and canonical ensembles. The focus is on the collective properties. Even at criticality the Nosé-Hoover thermostat (NHT) and dissipative particle dynamics thermostat (DPDT) provide results for diffusivities and shear viscosity that are in excellent agreement with the calculations in a microcanonical ensemble. However, while the DPDT appears to work well for bulk viscosity also, the NHT fails for this purpose.

The importance of the paper lies in the following fact. Very close to the critical point, for big enough systems, one needs extended simulation runs for the calculation of transport properties. In that case, for runs in microcanonical ensemble, it becomes difficult to avoid drift in temperature. Thus, the calculation of the transports in canonical ensemble may be of help. The NHT still being a very commonly used thermostat for the study of dynamics in the canonical ensemble, despite the criticisms about it, one needs to check its validity in situations as nontrivial as critical dynamics. It will be interesting to find out why the calculation for bulk viscosity via NHT is unreliable, despite the latter being a good one for other transport properties. One may argue, given that we have presented results only for $Q = 1$, if the value of Q is appropriately chosen, the NHT results for bulk viscosity may

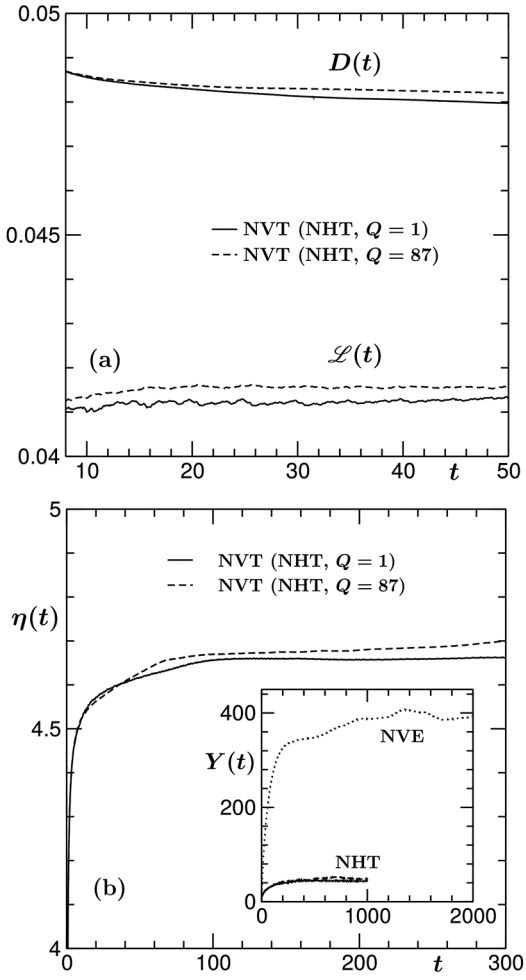

Fig. 7. (a) A comparative plot of $D(t)$ and $\mathscr{L}(t)$, obtained using NHT, for two values of Q. Results correspond to $L = 10$, $T = T_c^L$. Data for $\mathscr{L}$ has been multiplied by 3. (b) Same as (a), but for $\eta(t)$ (main frame) and $Y(t)$ (inset). For bulk viscosity we have included data from NVE ensemble as well.

match the numbers obtained from microcanonical simulations. In fig. 7, we demonstrate, as stated earlier, that improvements do not occur even when an optimum value of Q is chosen. In this figure, we present results for all the transport properties, *vs.* time, calculated at T_c^L for $L = 10$, using $Q = 1$ and 87, the latter number being approximately the optimum value for this quantity. Within statistical fluctuations, the results from both the values of Q are in nice agreement with each other, for all the quantities. For bulk viscosity, we have included a plot from calculations in NVE ensemble as well. This was done due to the following fact. While for all the other quantities, either in this paper or elsewhere [16], we have explored comparison between NHT and NVE results in close vicinity of the critical point, the same is missing for bulk viscosity. In fig. 6, the temperatures were chosen to be significantly higher than T_c, keeping the inferior temperature controlling ability of DPDT and other technical difficulties in the calculation of bulk viscosity in mind.

A criticism about NHT is that [18, 29, 30], if there is an external force, there is a problem with momentum conservation. Recently, such a problem is being taken care of [18, 29, 30] by introducing a further soft pair potential and relative velocities. Despite some deficiencies, even the basic NHT appears to provide a reasonable description of dynamics for a number of quantities, as seen here. Even for nonequilibrium dynamics we have observed [31] recently that this thermostat produces expected results.

On the other hand, despite its better ability to preserve hydrodynamics, DPDT does not appear to be very suitable for studies of dynamic critical phenomena because of the temperature control problem. In this context, a recent work by Gross and Varnik [32] should be discussed. For studying dynamic critical phenomena, these authors proposed a mesoscopic approach, based on the lattice Boltzmann method. In addition to accounting for hydrodynamic transport, this approach keeps the temperature inherently constant.

SKD and SR acknowledge financial support from the Department of Science and Technology, India, via Grant No SR/S2/RJN-13/2009. SR is grateful to the Council of Scientific and Industrial Research, India, for their research fellowship. The authors acknowledge correspondence with C. Pastorino and T. Kreer, as well as useful comments from an anonymous referee. SKD acknowledges financial support from Marie-Curie Action Plan of European Commission (FP7-PEOPLE-2013-IRSES Grant No. 612707, DIONICOS).

References

1. J. Zinn-Justin, Phys. Rep. **344**, 159 (2001).
2. H. Eugene Stanley, *Introduction to Phase Transitions and Critical Phenomena* (Oxford University Press, Oxford, 1971).
3. A. Onuki, *Phase Transition Dynamics* (Cambridge University Press, UK, 2002).
4. A. Onuki, Phys. Rev. E **55**, 403 (1997).
5. P.C. Hohenberg, B.I. Halperin, Rev. Mod. Phys. **49**, 435 (1977).
6. R.A. Ferrell, J.K. Bhattacharjee, Phys. Rev. Lett. **88**, 77 (1982).
7. G.A. Olchowy, J.V. Sengers, Phys. Rev. Lett. **61**, 15 (1988).
8. J. Luettmer-Strathmann, J.V. Sengers, G.A. Olchowy, J. Chem. Phys. **103**, 7482 (1995).
9. M.A. Anisimov, J.V. Sengers, in *Equations of State for Fluids and Fluid Mixtures*, edited by J.V. Sengers, R.F. Kayser, C.J. Peters, H.J. White Jr. (Elsevier, Amsterdam, 2000) p. 381.
10. H.C. Burstyn, J.V. Sengers, Phys. Rev. Lett. **45**, 259 (1980).
11. H.C. Burstyn, J.V. Sengers, Phys. Rev. A **25**, 448 (1982).
12. D.P. Landau, K. Binder, *A Guide to Monte Carlo Simulations in Statistical Physics* 3rd edition (Cambridge University Press, Cambridge, 2009).
13. D. Frenkel, B. Smit, *Understanding Molecular Simulations: From Algorithm to Applications* (Academic Press, San Diego, 2002).
14. M.P. Allen, D.J. Tildesley, *Computer Simulations of Liquids* (Clarendon, Oxford, 1987).
15. D.C. Rapaport, *The Art of Molecular Dynamics Simulations* (Cambridge University Press, Cambridge, UK, 2004).
16. S. Roy, S.K. Das, J. Chem. Phys. **141**, 234502 (2014).
17. G.S. Grest, K. Kremer, Phys. Rev. A **33**, 3628 (1986).
18. S.D. Stoyanov, R.D. Groot, J. Chem. Phys. **122**, 114112 (2005).
19. P. Nikunen, M. Karttunen, I. Vattulainen, Comput. Phys. Commun. **153**, 407 (2003).
20. T. Soddemann, B. Dünweg, K. Kremer, Phys. Rev. E **68**, 046702 (2003).
21. C. Pastorino, T. Kreer, M. Müller, K. Binder, Phys. Rev. E **76**, 026706 (2007).
22. S.K. Das, M.E. Fisher, J.V. Sengers, J. Horbach, K. Binder, Phys. Rev. Lett. **97**, 025702 (2006).
23. S.K. Das, J. Horbach, K. Binder, M.E. Fisher, J.V. Sengers, J. Chem. Phys. **125**, 024506 (2006).
24. S. Roy, S.K. Das, EPL **94**, 36001 (2011).
25. S. Roy, S.K. Das, J. Chem. Phys. **139**, 064505 (2013).
26. J.-P. Hansen, I.R. McDonald, *Theory of Simple Liquids* (Academic Press, London, 2008).
27. S. Nosé, Prog. Theor. Phys. **103**, 1 (1991).
28. M.E. Fisher, in *Critical Phenomena*, edited by M.S. Green (Academic Press, London, 1971) p. 1.
29. M.P. Allen, F. Schmid, Mol. Simul. **33**, 21 (2007).
30. X. Yong, L.T. Zhang, J. Chem. Phys. **138**, 084503 (2013).
31. S. Roy, S.K. Das, Phys. Rev. E **85**, 050602 (2012).
32. M. Gross, F. Varnik, Phys. Rev. E **86**, 061119 (2012).